Volume 58
Number 23
21 March 2022
Pages 3707–3836

ChemComm

Chemical Communications

rsc.li/chemcomm

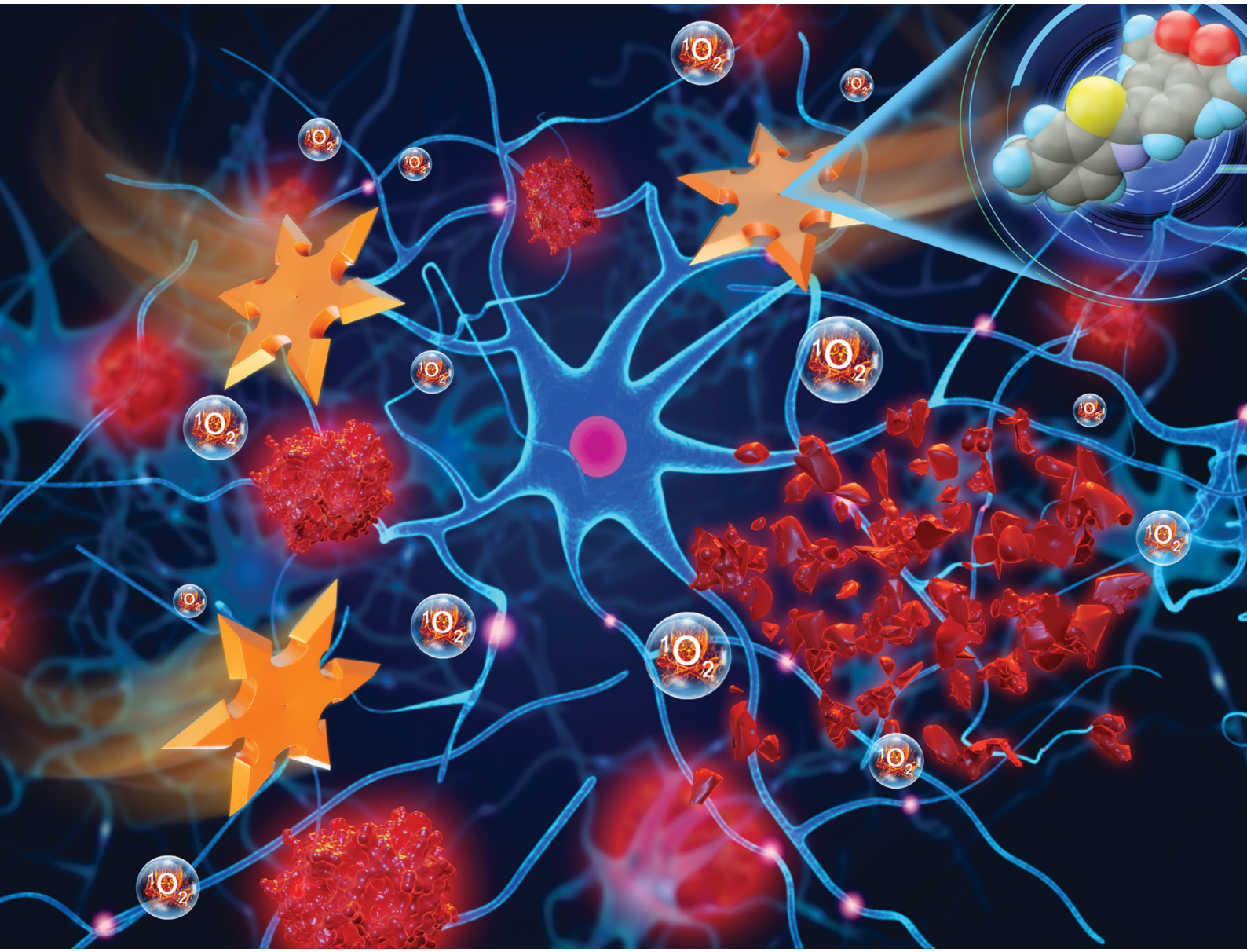

ISSN 1359-7345

ROYAL SOCIETY OF CHEMISTRY

COMMUNICATION

Lei Wang, Engin U. Akkaya *et al.*
Degradation of amyloid peptide aggregates by targeted singlet oxygen delivery from a benzothiazole functionalized naphthalene endoperoxide

ChemComm

COMMUNICATION

View Article Online
View Journal | View Issue

Check for updates

Cite this: *Chem. Commun.*, 2022, 58, 3747

Received 20th December 2021,
Accepted 11th January 2022

DOI: 10.1039/d1cc07133e

rsc.li/chemcomm

Degradation of amyloid peptide aggregates by targeted singlet oxygen delivery from a benzothiazole functionalized naphthalene endoperoxide†

Hao Wu, Ziang Liu, Yujie Shao, Guangzhe Li, Yue Pan, Lei Wang* and Engin U. Akkaya*

Aggregate structures formed by amyloid-β (Aβ) are correlated with the progression of pathogenesis in Alzheimer's disease. Previous works have shown that photodynamic photosensitizers were effective in oxidatively degrading amyloid-β aggregates and thus decreasing their cytotoxicity under various conditions. In this work, we designed and synthesized a benzothiazole–naphthalene conjugate, with high level of structural analogy to Thioflavin T which is known to have high affinities for the amyloid peptide aggregates. The endoperoxide form (BZTN-O_2) of this compound, which releases singlet oxygen with a half-life of 77 minutes at 37 °C, successfully inhibited and/or reversed amyloid aggregation. The endoperoxide is capable of singlet oxygen release without any need for light, and its charge-neutral form could allow blood–brain barrier (BBB) permeability. The therapeutic potential of such endoperoxide compounds with amyloid binding affinity is exciting.

Open Access Article. Published on 24 January 2022. Downloaded on 12/5/2025 8:44:44 AM.
This article is licensed under a Creative Commons Attribution 3.0 Unported Licence.

Alzheimer's disease (AD) is the most common form of dementia.[1] The discovery of amyloid beta (Aβ) plaques in the extracellular space of the brains of AD patients in 1984, led to the "amyloid hypothesis".[2] This hypothesis posits that Aβ monomers assemble into toxic oligomers and fibrous aggregates, causing neuronal damage. Resulting clinical symptoms are cognitive disfunction and memory loss. In addition to Aβ plaques, neurofibrillary tangles (NFT) composed of tau protein are correlated with cognitive disfunction.[3] In one model of AD initiation/progression, Aβ is the trigger and NFT are the bullets for neurotoxicity.[4]

While AD has been linked to oxidative stress and reactive oxygen species (ROS),[5] the process requires finer assessment of the roles of individual ROS and/or reactive nitrogen species (RNS) entities, and not appropriate for painting with a broad brush. In fact, a number of articles appeared recently,[5] clearly demonstrating the fact that the oxygenation of amyloid peptides under the conditions of photodynamic action reduced their neurotoxicity. Furthermore, using Drosophila AD models two different photosensitizers resulted in full recovery of the locomotion defects.[5f,g] The photosensitized reaction is highly specific, and the most important change is the oxidation of a methionine residue at the position 35 (M35) of the $A\beta_{42}$ peptide.[5b] This particular amino acid is critical for holding the conformation needed for aggregation of Aβ peptides into toxic oligomers and fibril structures, and its oxidation to methionine sulfoxide inhibits the rate of aggregation.[6] The reactivity and the mode of generation suggest that singlet oxygen is involved in the oxidation reactions.[7] In fact, it is known that singlet oxygen effectively reacts with methionine residues to yield sulfoxide.[7]

Photodynamic generation of singlet oxygen suffers from two inherent limitations, light cannot be transmitted through tissues effectively,[8] especially through the skull,[9] in the case of brain tissues. Also, photodynamic singlet oxygen generation depletes local oxygen resources. Based on our previous experience with on target, and on demand delivery of singlet oxygen, we set out to design and synthesize an Aβ binding compound with endoperoxide moieties which could thermally release singlet oxygen to disrupt Aβ oligomerization and aggregation. To that end, we noted that Thioflavin T (Fig. 1) is known to be a selective fluorescent stain for Aβ fibril structures. On binding, the fluorescence emission near 480 nm is significantly enhanced. Well-known ^{11}C PET tracer "Pittsburgh compound B" (a.k.a. **PiB**, or **BTA-1**) is structurally related to **ThT**, and it is highly selective for amyloid β deposits in brain.

The simple naphthalene derivative **BZTN** and its endoperoxide form **BZTN-O_2** were designed in an attempt to keep maximum structural similarity to **ThT** and **PiB** while introducing an endoperoxide module. The synthesis of the target compounds (Fig. 2) starts with 1,4-dimethylnaphthalene (**1**). Functionalization at the 6 positions was done by following a

State Key Laboratory of Fine Chemicals, and Department of Pharmaceutical Science, Dalian University of Technology, 2 Linggong Road, 116024 Dalian, China. E-mail: eua@dlut.edu.cn, leiwang@dlut.edu.cn

† Electronic supplementary information (ESI) available: Experimental section outlining synthetic procedures, characterization data, kinetic studies and cell studies as well as supplementary figures. See DOI: 10.1039/d1cc07133e

Open Access Article. Published on 24 January 2022. Downloaded on 12/5/2025 8:44:44 AM.
This article is licensed under a Creative Commons Attribution 3.0 Unported Licence.

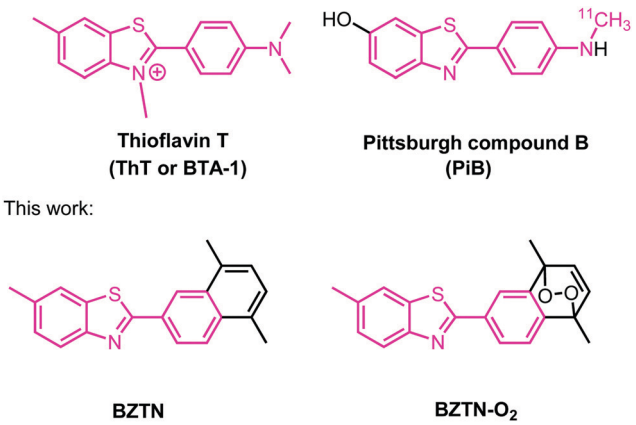

Fig. 1 Structures of Thioflavin T and the ^{11}C-labeled PET imaging agent Pittsburgh compound B. In this work, the compounds **BZTN** and **BZTN-O$_2$** were synthesized.

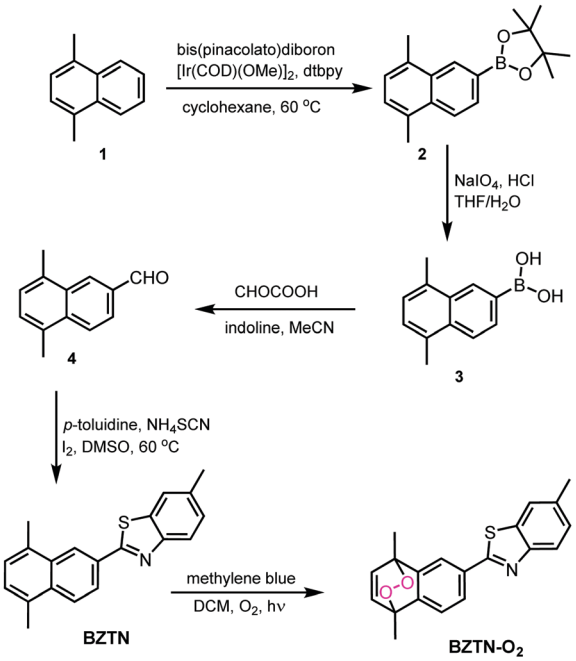

Fig. 2 Synthesis path for the compounds **BZTN** and its endoperoxide **BZTN-O$_2$**.

useful regioselective borylation reported by the Suginome group.[10] Deprotection of the compound 2 was carried out according to literature, followed by conversion of the boronic acid functionality to a formyl group by a modified Petasis reaction.[11] Benzothiazole core was then generated by the reaction of the aldehyde with *p*-toluidine, thiocyanate and iodine in DMSO. **BZTN** obtained in this way can conveniently be transformed into endoperoxide **BZTN-O$_2$**, by the reaction of singlet oxygen obtained by photosensitization.

The cycloreversion reaction rate of the endoperoxide **BZTN-O$_2$** was determined following the changes in the ^1H NMR of the compound in $CDCl_3$. The first order reaction

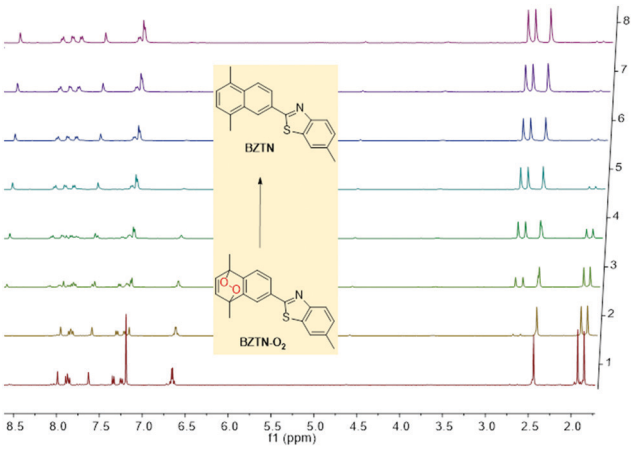

Fig. 3 Temporal evolution of **BZTN-O$_2$** ^1H NMR in $CDCl_3$ at 37 °C. It is noteworthy that conversion is back to **BZTN** in a clean reaction without any by-products.

rate and the half-life of the endoperoxide can be obtained by following the changes in the integral ratios of the various peaks, such as essentially unchanged singlet methyl peak of the benzothiazole core near 2.45 ppm *versus* the two new singlet peaks appearing near 2.7 ppm (Fig. 3).

The half-life at 37 °C was determined to be 77 minutes which is in the expected range for most naphthalene endoperoxides.[12] We then proceeded to establish that the other product is indeed singlet oxygen by carrying out the cycloreversion reaction of the endoperoxide **BZTN-O$_2$** (Fig. 4) in the presence of singlet oxygen trap 1,3-diphenylisobenzofuran (DPBF).

In order to assess the utility of the **BZTN-O$_2$** in degradation of the Aβ aggregates we have carried out following experiments. First, a solution of monomeric $A\beta_{1-42}$ was prepared in hexafluoro-2-propanol (HFIP) and kept at room temperature overnight. The solution was divided into aliquots desiccated to afford film-like lyophilized $A\beta_{1-42}$. For the ThT binding assay (ESI) $A\beta_{1-42}$ film was re-dissolved in ammonium hydroxide solution, then diluted with phosphate buffer. A mixture of the peptide (50 μM, final concentration) with or without **BZTN** or

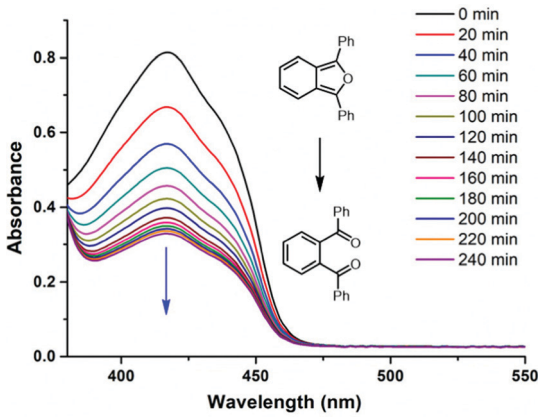

Fig. 4 The decrease in the absorption peak of DPBF (50 μM) in the presence of **BZTN-O$_2$** (500 μM) in DMSO in dark at 37 °C.

 This journal is © The Royal Society of Chemistry 2022

Open Access Article. Published on 24 January 2022. Downloaded on 12/5/2025 8:44:44 AM.
This article is licensed under a Creative Commons Attribution 3.0 Unported Licence.

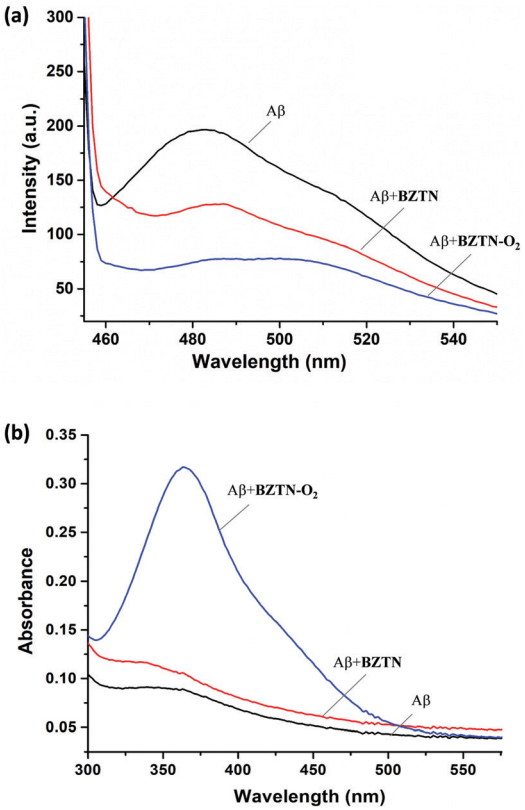

Fig. 5 (a) **ThT** emission spectra following typical assay procedure for the Aβ, Aβ + **BZTN** and Aβ + **BZTN-O$_2$** samples. Excitation at 450 nm. (b) Absorption spectra obtained following DNPH assay procedures for the Aβ, Aβ + **BZTN** and Aβ + **BZTN-O$_2$** samples. **BZTN-O$_2$** results in significant oxidative transformations.

BZTN-O$_2$ (100 μM) was incubated at 37 °C for 48 h. After incubation, **ThT** (5 μM) was added. Then the fluorescence intensities were recorded after five minutes. ThT specific for β-sheet aggregate structures and our data shows that **BZTN-O$_2$** very effectively inhibits formation of these structures (Fig. 5a) as evidenced by the decrease of emission intensity. The inhibitory effect of the **BZTN** itself is also expected as it is capable of binding the β-sheet rich aggregates.

Another assay commonly used to assess oxidative transformation of peptides is the chromogenic 2,4-dinitrophenylhydrazine (DNPH) assay. Aβ_{1-42} in solution was precipitated with a trichloroacetic acid (TCA, 20% final concentration) solution at 0 °C, the peptide was then collected by centrifugation. DNPH was added (10 mM DNPH in 2.0 M of HCl) followed by 1 h incubation at room temperature. The samples processed further and finally absorption spectra were collected (Fig. 5b). As expected, +**BZTN-O$_2$** results in large hydrazone peak unlike +**BZTN** or Aβ alone, which is clearly due to singlet oxygen mediated side chain oxidation. The process is selective, under the same conditions, BSA is oxidized only to a small extent (ESI,† Fig. S2).

Finally, we wanted observe the changes in the amyloid fibrils and aggregate structures microscopically (TEM) compared various control cases, including curcumin, well-known[13] disruptor of amyloid aggregation (ESI†). To that end, Aβ_{1-42} peptide stock

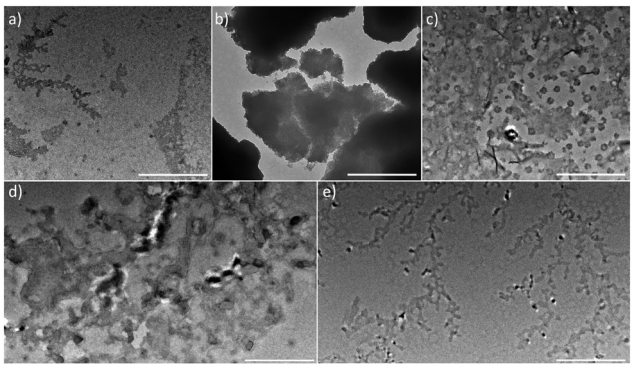

Fig. 6 TEM images acquired for the samples subjected to following conditions: (a) 25 μM Aβ_{1-42} alone t = 0 h (b) 25 μM Aβ_{1-42} alone, 48 h incubation at 37 °C; (c) 25 μM Aβ_{1-42} and 25 μM curcumin 48 h incubation at 37 °C; (d) 25 μM Aβ_{1-42} and 25 μM **BZTN** 48 h incubation at 37 °C; (e) 25 μM Aβ_{1-42} and 25 μM **BZTN-O$_2$** 48 h incubation at 37 °C. Bar 500 nm.

was diluted with phosphate buffer (pH 7.4) to 100 μM before use. For the inhibition of Aβ_{1-42} aggregation, monomeric Aβ_{1-42} was incubated with **BZTN-O$_2$**, **BZTN** or curcumin at 37 °C for 48 h, respectively. Monomeric Aβ_{1-42} and aggregated Aβ_{1-42} were used as control groups. The concentration of Aβ_{1-42} and the test compounds were set as 25 μM (final concentration). Aliquots of the samples were placed on a carbon coated copper/rhodium grid and each grid was stained with 0.5% phosphotungstate solution for 2 min. The excess staining solution was removed and the specimen was transferred for imaging with transmission electron microscopy. Images acquired (Fig. 6) show that 37 °C incubation results in in large aggregate structures (Fig. 6b) whereas curcumin only leads to small globular structures (Fig. 6c). Compound **BZTN** is less effective (Fig. 6d) than curcumin, but **BZTN-O$_2$** (Fig. 6e) inhibits aggregate structures altogether.

Similar experiments where **BZTN-O2** is added after the aggregation, also showed effective degradation of the preformed aggregate structures (ESI,† Fig. S7) as evidenced by TEM images.

AFM images were also acquired (Fig. 7) for samples of Aβ_{1-42} exposed to **BZTN-O2**. Large aggregate structures were successfully degraded in the presence of 25 μM.

Finally, toxicity of the compounds was assessed using two normal cell cultures. We are pleased to report (Fig. 8) that within the concentration range of our study, both **BZTN** and **BZTN-O2** are not cytotoxic.

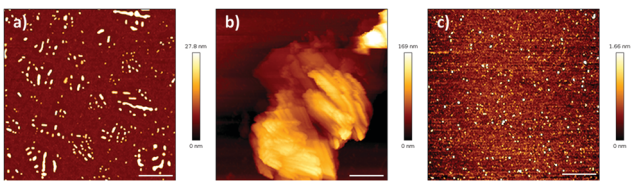

Fig. 7 AFM images acquired for the samples subjected to following conditions: (a) 25 μM Aβ_{1-42} alone t = 0 h (b) 25 μM Aβ_{1-42} alone, 48 h incubation at 37 °C; (c) 25 μM Aβ_{1-42} and 25 μM **BZTN-O$_2$** 48 h incubation at 37 °C. Bar 2 μm.

Open Access Article. Published on 24 January 2022. Downloaded on 12/5/2025 8:44:44 AM.
This article is licensed under a Creative Commons Attribution 3.0 Unported Licence.

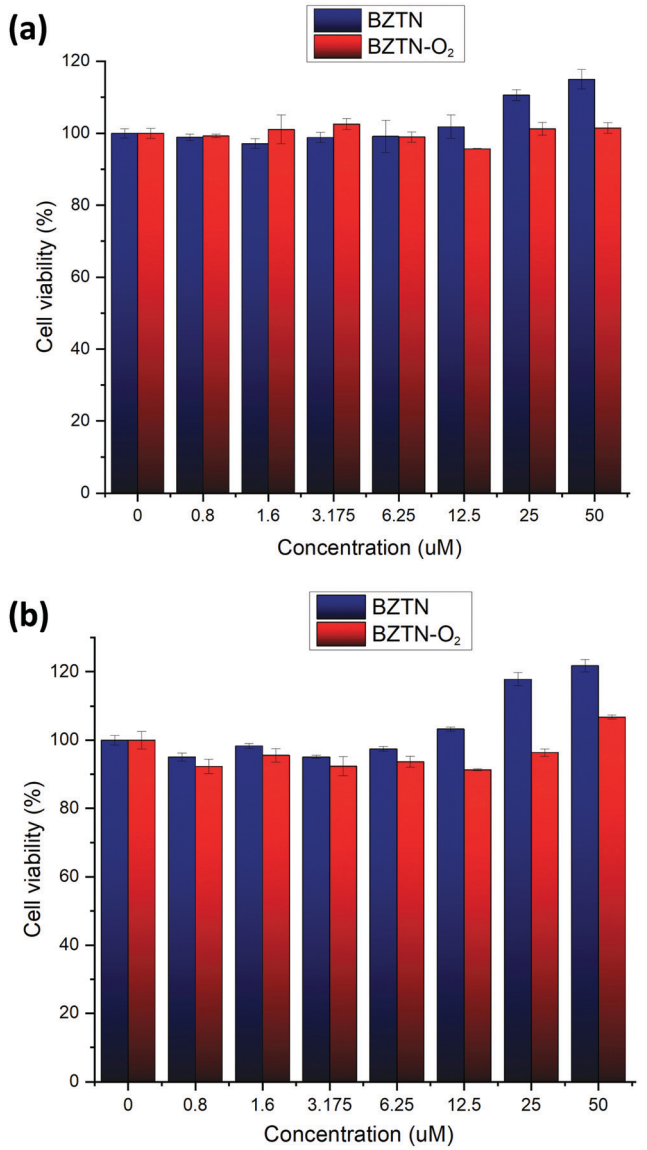

Fig. 8 Cytotoxicity of **BZTN** and **BZTN-O$_2$** against (a) HUVEC (b) L02 cell cultures.

In conclusion, we were able to demonstrate that an endoperoxide with an affinity to amyloid beta clusters, is capable of inhibiting aggregation *via* oxidative transformation. The therapeutic potential of this, and conceptually related compounds are currently under study in our laboratories.

The authors acknowledge financial support from LiaoNing Revitalization Talents Program (E. U. A.: XLYC1902001, L. W.: XLYC1907021) and the National Science Foundation of China (L. W.: 22007008).

Conflicts of interest

There are no conflicts to declare.

Notes and references

1 A. Burns and S. Iliffe, *BMJ*, 2009, **338**, 405–409.
2 (*a*) D. J. Selkoe, *Neuron*, 1991, **6**, 487–489; (*b*) J. A. Hardy and G. A. Higgins, *Science*, 1992, **256**, 184–185.
3 (*a*) H. Braak and E. Braak, *Acta Neuropathol.*, 1991, **82**, 239–259; (*b*) L. M. Ittner and J. Götz, *Nat. Rev. Neurosci.*, 2011, **12**, 67–72.
4 G. S. Bloom, *JAMA Neurol.*, 2014, **71**, 505–508.
5 (*a*) H. Yagi, D. Ozawa, K. Sakurai, T. Kawakami, H. Kuyama, O. Nishimura, T. Shimanouchi, R. Kuboi, H. Naiki and Y. Goto, *J. Biol. Chem.*, 2010, **285**, 19660–19667; (*b*) A. Taniguchi, Y. Shimizu, K. Oisaki, Y. Sohma and M. Kanai, *Nat. Chem.*, 2016, **8**, 974–982; (*c*) A. Taniguchi, D. Sasaki, A. Shiohara, T. Iwatsubo, T. Tomita, Y. Sohma and M. Kanai, *Angew. Chem., Int. Ed.*, 2014, **53**, 1382–1385; (*d*) J. S. Lee, B. I. Lee and C. B. Park, *Biomaterials*, 2015, **38**, 43–49; (*e*) A. Hirabayashi, Y. Shindo, K. Oka, D. Takahashi and K. Toshima, *Chem. Commun.*, 2014, **50**, 9543–9546; (*f*) B. I. Lee, S. Lee, Y. S. Suh, J. S. Lee, A.-K. Kim, O. Y. Kwon, K. Yu and C. B. Park, *Angew. Chem., Int. Ed.*, 2015, **54**, 11472–11476; (*g*) B. I. Lee, Y. S. Suh, Y. J. Chung, K. Yu and C. B. Park, *Sci. Rep.*, 2017, **7**, 752; (*h*) Y.-J. Hsieh, K.-Y. Chien, I.-F. Yang, I.-N. Lee, C.-C. Wu, T.-Y. Huang and J.-S. Yu, *Sci. Rep.*, 2017, **7**, 1370; (*i*) M. W. Beck, J. S. Derrick, R. A. Kerr, S. B. Oh, W. J. Cho, S. J. C. Lee, Y. Ji, J. Han, Z. A. Tehrani, N. Suh, S. Kim, S. D. Larsen, K. S. Kim, J.-Y. Lee, B. T. Ruotolo and M. H. Lim, *Nat. Commun.*, 2016, **7**, 13115.
6 (*a*) L. Hou, I. Kang, R. E. Marchant and M. G. Zagorski, *J. Biol. Chem.*, 2002, **277**, 40173–40176; (*b*) L. Hou, H.-G. Lee, F. Han, J. M. Tedesco, G. Perry, M. A. Smith and M. G. Zagorski, *J. Alzheimer's Dis.*, 2013, **37**, 9–18.
7 (*a*) Y. Yan, S. A. McCallum and C. Wang, *J. Am. Chem. Soc.*, 2008, **130**, 5394–5395; (*b*) M. Liu, E. Ucar, Z. Liu, L. Wang, L. Yang, J. Xu and E. U. Akkaya, *RSC Adv.*, 2021, **11**, 14513–14516; (*c*) F. Liu, W. Lu, X. Yin and J. Liu, *J. Am. Soc. Mass Spectrom.*, 2016, **27**, 59–72.
8 S. Stolik, J. A. Delgado, A. Perez and L. Anasagasti, *J. Photochem. Photobiol., B*, 2000, **57**, 90–93.
9 (*a*) P. A. Lapchak, P. D. Boitano, P. V. Butte, D. J. Fisher, T. Hölscher, E. J. Ley, M. Nuño, A. H. Voie and P. S. Rajput, *PLoS One*, 2015, **10**, e0127580; (*b*) F. Salehpour, P. Cassano, N. Rouhi, M. R. Hamblin, L. De Taboada, F. Farajdokht and J. Mahmoudi, *Photobiomodulation, Photomed., Laser Surg.*, 2019, **37**, 581–595.
10 T. Yamamoto, A. Ishibashi, M. Koyanagi, H. Ihara, N. Eichenauer and M. Suginome, *Bull. Chem. Soc. Jpn.*, 2017, **90**, 604–606.
11 H. Huang, C. Yu, X. Li, Y. Zhang, Y. Zhang, X. Chen, P. S. Mariano, H. Xie and W. Wang, *Angew. Chem., Int. Ed.*, 2017, **56**, 8201–8205.
12 (*a*) M. Klapper and T. Linker, *Chem. – Eur. J.*, 2015, **21**, 8569–8577; (*b*) E. Ucar, D. Xi, O. Seven, C. Kaya, X. J. Peng, W. Sun and E. U. Akkaya, *Chem. Commun.*, 2019, **55**, 13808–13811; (*c*) M. Qu, N. Wu, W. Q. Jiang, L. Wang, M. S. Akkaya and E. U. Akkaya, *RSC Adv.*, 2021, **11**, 19083–19087.
13 F. Yang, G. P. Lim, A. N. Begum, O. J. Ubeda, M. R. Simmons, S. S. Ambegaokar, P. P. Chen, R. Kayed, C. G. Glabe, S. A. Frautschy and G. M. Cole, *J. Biol. Chem.*, 2005, **280**, 5892–5901.

 This journal is © The Royal Society of Chemistry 2022